The Journal of Chemical Physics

Non-Hermitian cavity quantum electrodynamics–configuration interaction singles approach for polaritonic structure with *ab initio* molecular Hamiltonians

Cite as: J. Chem. Phys. **156**, 154103 (2022); https://doi.org/10.1063/5.0091953
Submitted: 18 March 2022 • Accepted: 27 March 2022 • Accepted Manuscript Online: 31 March 2022 • Published Online: 18 April 2022

Jonathan McTague and Jonathan J. Foley

View Online Export Citation CrossMark

ARTICLES YOU MAY BE INTERESTED IN

Simulating photodissociation reactions in bad cavities with the Lindblad equation
The Journal of Chemical Physics **153**, 234304 (2020); https://doi.org/10.1063/5.0033773

A general implementation of time-dependent vibrational coupled-cluster theory
The Journal of Chemical Physics **153**, 234109 (2020); https://doi.org/10.1063/5.0034013

Cavity-modulated ionization potentials and electron affinities from quantum electrodynamics coupled-cluster theory
The Journal of Chemical Physics **154**, 094112 (2021); https://doi.org/10.1063/5.0038748

Lock-in Amplifiers up to 600 MHz
Zurich Instruments
Watch

© 2022 Author(s).

The Journal of Chemical Physics ARTICLE scitation.org/journal/jcp

Non-Hermitian cavity quantum electrodynamics–configuration interaction singles approach for polaritonic structure with *ab initio* molecular Hamiltonians

Cite as: J. Chem. Phys. 156, 154103 (2022); doi: 10.1063/5.0091953
Submitted: 18 March 2022 • Accepted: 27 March 2022 •
Published Online: 18 April 2022

View Online Export Citation CrossMark

Jonathan McTague and Jonathan J. Foley IV[a)]

AFFILIATIONS

William Paterson University, Department of Chemistry, 300 Pompton Road, Wayne, New Jersey 07470, USA

Note: This paper is part of the 2022 JCP Emerging Investigators Special Collection.
[a)]**Electronic mail:** foleyj10@wpunj.edu

ABSTRACT

We combine *ab initio* molecular electronic Hamiltonians with a cavity quantum electrodynamics model for dissipative photonic modes and apply mean-field theories to the ground- and excited-states of resulting polaritonic systems. In particular, we develop a non-Hermitian configuration interaction singles theory for mean-field ground- and excited-states of the molecular system strongly interacting with a photonic mode and apply these methods to elucidating the phenomenology of paradigmatic polaritonic systems. We leverage the Psi4Numpy framework to yield open-source and accessible reference implementations of these methods.

© 2022 Author(s). All article content, except where otherwise noted, is licensed under a Creative Commons Attribution (CC BY) license (http://creativecommons.org/licenses/by/4.0/). https://doi.org/10.1063/5.0091953

I. INTRODUCTION

The interaction between molecular excitations and nanoconfined photons can produce the requisite strong interactions for polaritonic chemistry.[1–32] Motivated by a desire to provide a realistic picture of the molecular structure under the influence of strong photonic interaction, there has been a recent surge in the activity focused on merging *ab initio* molecular electronic structure theory with cavity quantum electrodynamics (*ab initio* CQED) to provide an accurate and predictive model of polaritonic chemistry.[11,26,29,33–38] Such efforts include combining CQED with density functional theory (DFT) or its time-dependent extension (TDDFT),[33,38–42] reduced density matrix mechanics,[37] and wavefunction theory using the coupled-cluster ansatz.[26,29,31,36] These approaches can provide access to potential energy surfaces, couplings, and other properties of interest for simulating the structure and the reactivity of polaritonic chemical systems.

The role of photonic dissipation or cavity losses on polaritonic structure and dynamics has recently been discussed in a number of studies utilizing model Hamiltonians,[20,25,27,32] although, to our knowledge, the effort to pursue *ab initio* CQED methods has not explicitly included photonic loss. In this context, photonic dissipation refers to the finite lifetime of occupied photonic modes that exist within a cavity. Photonic dissipation occurs because the photons confined within a cavity can couple to the material degrees of freedom that exist in the cavity itself (which can be significant when considering plasmonic cavities), and also to the continuum of modes that exist outside the cavity (which causes leakage of photons in Fabry–Perot cavities, for example).[20,27,43] In this work, we present a simple *ab initio* CQED method for treating ground and excited polaritonic states with explicit inclusion of photonic lifetimes via a non-Hermitian cavity quantum electrodynamics–configuration interaction singles approach (NH-CQED-CIS). This approach provides a simplification for the couplings between photon and material degrees of freedom that contribute to photon dissipation and subsumes these complicated interactions into a complex frequency of the photon that quantifies the sum of all photon dissipation rates.[27,43] Setting the imaginary part of the frequency to zero in this approach implies a lossless photonic mode that is perfectly isolated from the environment and returns the formulation to a Hermitian

© Author(s) 2022

CQED-CIS theory. We implement this approach in the coherent state basis that results from the solution of the CQED-Hartree-Fock (CQED-HF) equations. Both the Hermitian and non-Hermitian formulations of CQED-CIS in the CQED-HF basis contain additional couplings to the CQED-HF reference which are not present in canonical CIS theory, and as a result, our method also provides both ground- and excited-states information about the molecular system coupled to a cavity mode. We endeavor to provide a detailed picture of the key equations and algorithmic considerations for both the CQED-HF and NH-CQED-CIS approaches and, therefore, provide detailed equations of NH-CQED-CIS in the main text, detailed equations for CQED-HF in Appendixes A–C, and reference implementations of both methods through the Psi4Numpy project.[44] We apply both methods to the analysis of several paradigmatic systems, including the ground-state polaritonic structure of formaldehyde coupled to cavity modes that can modify the symmetry of the ground-state wavefunction and the polaritonic potential energy surfaces of the magnesium hydride ion coupled to a lossy photonic mode. We also compute the approximate photon occupation of ground-state obtained from NH-CQED-CIS in the ultra-strong coupling regime for a variety of loss rates, showing qualitative agreement with the analysis found in Ref. 6.

II. THEORY

We start with the Pauli–Fierz Hamiltonian in the dipole approximation in the length gauge, written in atomic units, following Refs. 26, 29, and 34,

$$\hat{H} = \hat{H}_e + \hat{H}_p + \hat{H}_{dse} + \hat{H}_{ep}, \tag{1}$$

where

$$\hat{H}_e = \sum_{i}^{N_e} \hat{T}_e(x_i) + \sum_{i}^{N_e}\sum_{A}^{N_N} \hat{V}_{eN}(x_i; X_A) + \sum_{i}^{N_e}\sum_{j}^{N_e} \hat{V}_{ee}(x_i, x_j) + V_{NN}, \tag{2}$$

with $\hat{T}_e(x_i)$ denoting the electronic kinetic energy operator for electron i, $\hat{V}_{eN}(x_i; X_A)$ being the (attractive) coulomb operator for electron i and nucleus A, $\hat{V}_{ee}(x_i, x_j)$ being the (repulsive) coulomb operator for electrons i and j, and V_{NN} being the total (repulsive) coulomb potential between all of the nuclei. Within the Born–Oppenheimer approximation, V_{NN} is a constant, the nuclear kinetic energy is neglected, and the electron-nuclear attraction depends parametrically on the fixed nuclear coordinates. The photonic contribution is captured by the complex energy,

$$\hat{H}_p = \tilde{\omega}\hat{b}^\dagger\hat{b}, \tag{3}$$

and the photon–molecule interaction contains a bilinear coupling term,

$$\hat{H}_{ep} = -\sqrt{\frac{\tilde{\omega}}{2}}(\lambda \cdot (\hat{\mu} - \langle\mu\rangle))\left(\hat{b}^\dagger + \hat{b}\right), \tag{4}$$

and a quadratic dipole self-energy term,

$$\hat{H}_{dse} = \frac{1}{2}(\lambda \cdot (\hat{\mu} - \langle\mu\rangle))^2. \tag{5}$$

In the above-mentioned equations, $\hat{b}^\dagger$ and $\hat{b}$ are the bosonic raising and lowering operators for the photonic degrees of freedom, respectively, and $\tilde{\omega} = \omega - i\frac{\gamma}{2}$ is a complex frequency of the photon, with the real part ω being related to the energy of the photon and the imaginary part $\gamma/2$ being related to the dissipation rate of the photonic degree of freedom.[20,27,43] The term $\langle\mu\rangle$ represents the ground-state molecular dipole expectation value, which has the Cartesian components, ξ, where $\xi \in \{x, y, z\}$. A given ξ-component of the dipole operator has the form $\hat{\mu}^\xi = \sum_i^{N_e}\hat{\mu}^\xi(x_i) + \mu^\xi_{nuc}$, where $\hat{\mu}^\xi(x_i)$ is an operator that depends on electronic coordinates, and within the Born–Oppenheimer approximation, we treat the Cartesian components of the nuclear dipole moment μ^ξ_{nuc} as functions of the nuclear coordinates rather than a quantum mechanical operator. Note that the shift of the Hamiltonian by $\langle\mu\rangle$ results from the transformation to the coherent state basis.[26] In the presented NH-CQED-CIS theory, we will utilize an orbital basis that arises from solving the CQED-RHF equations arising from a Hermitian total Hamiltonian, where only the real part of $\tilde{\omega}$ is retained. The CQED-RHF method has been described elsewhere,[26,29] although we provide a brief outline in Appendixes A–C. Also, provided in Appendixes A–C is an expansion of the $\hat{H}_{dse}$ term that explicitly shows where the one-electron dipole, one-electron quadrupole, and two-electron dipole operator terms that appear in the NH-CQED-CIS matrix elements come from. We also note that the formulation presented here considers only a single photonic mode; generalizations to multiple photonic modes can be formulated by introducing additional frequencies and coupling parameters for each additional modes in the $\hat{H}_p$, $\hat{H}_{ep}$, and $\hat{H}_{dse}$ terms. In particular, the multimode version would read as $\hat{H}_p = \sum_i \tilde{\omega}_i \hat{b}_i^\dagger \hat{b}_i$, $\hat{H}_{ep} = -\sum_i \sqrt{\frac{\tilde{\omega}_i}{2}}(\lambda_i \cdot (\hat{\mu} - \langle\mu\rangle))\left(\hat{b}_i^\dagger + \hat{b}_i\right)$, and $\hat{H}_{dse} = \sum_i \frac{1}{2}(\lambda_i \cdot (\hat{\mu} - \langle\mu\rangle))^2$.

A mean-field description of the excited-states of the molecular system strongly interacting with photonic degrees of freedom, and a correction to the ground-state that contains coupling between the CQED-RHF reference and simultaneous electronic and photonic excitations, may be obtained through a configuration interaction singles (CIS) ansatz. Here, we formulate a non-Hermitian version of such an ansatz, NH-CQED-CIS, that incorporates the dissipative features of the photonic degrees of freedom. In our presentation, we formulate NH-CQED-CIS in the coherent state basis by using the orbitals that result from the CQED-RHF approach outlined in Appendixes A–C.

The polaritonic energy eigenfunctions for state I in the NH-CQED-CIS ansatz can be written as a linear combination of the CQED-RHF reference and the products of all possible single electron excitations out of the CQED-RHF reference. The CQED-RHF reference involves the product of an electronic Slater determinant with the photon vacuum state $|\Phi_o\rangle|0\rangle$, so single excitations can occur as electronic excitations from an occupied orbital ϕ_i to a virtual orbital ϕ_a, the raising of the photon number state from $|0\rangle \rightarrow |1\rangle$, or both. We, therefore, write the NH-QED-CIS wavefunction for state I as

$$\Psi_I = c_0^0|\Phi_0\rangle|0\rangle + c_0^1|\Phi_0\rangle|1\rangle + \sum_{i,a} c_{ia}^0|\Phi_i^a\rangle|0\rangle + \sum_{i,a} c_{ia}^1|\Phi_i^a\rangle|1\rangle, \tag{6}$$

© Author(s) 2022

where the coefficients c denote the contribution of a given term to the wavefunction and we have denoted the electronic excitations in the subscript and the photonic excitations in the superscript of these coefficients. For the case of multiple modes, the photonic basis states will be augmented to consider all possible combinations of the occupations of those modes within a maximum photon number. These coefficients, and the corresponding energy eigenvalues for a given NH-CQED-CIS state I, may be obtained by diagonalizing the Hamiltonian matrix built in the basis shown in Eq. (6). We spin adapt this basis such that $|\Phi_i^a\rangle = \frac{1}{\sqrt{2}}\left(|\Phi_{i\alpha}^{a\alpha}\rangle + |\Phi_{i\beta}^{a\beta}\rangle\right)$, where α and β label the spin orbitals as being occupied by spin-up and spin-down electrons, respectively. There are three classes of matrix elements that contribute to the Hamiltonian matrix, and we write each class of matrix elements after shifting the total Hamiltonian in Eq. (1) by $E_{CQED-RHF}$. The matrix elements involving the CQED-RHF electronic Slater determinant $|\Phi_0\rangle$ and photonic states $|s\rangle$ and $|t\rangle$, where $s, t \in \{0, 1\}$, involve only the (complex) photonic energy,

$$\langle s|\langle\Phi_0|\hat{H} - E_{CQED-RHF}|\Phi_0\rangle|t\rangle = \tilde{\omega}\, t\delta_{st}. \tag{7}$$

Matrix elements coupling $|\Phi_0\rangle|s\rangle$ to $|\Phi_i^a\rangle|t\rangle$ involve only the $\hat{H}_{ep}$ contributions,

$$\langle s|\langle\Phi_0|\hat{H} - E_{CQED-RHF}|\Phi_i^a\rangle|t\rangle = -\sqrt{\tilde{\omega}}\sqrt{t+1}\delta_{s,t+1}\sum_\xi \lambda^\xi \mu_{ia}^\xi - \sqrt{\tilde{\omega}}\sqrt{t}\delta_{s,t-1}\sum_\xi \lambda^\xi \mu_{ia}^\xi. \tag{8}$$

Matrix elements coupling different singly excited electronic and/or photonic states involve all terms of the Hamiltonian, including the canonical CIS terms,

$$\begin{aligned}\langle s|\langle\Phi_i^a|\hat{H} - E_{CQED-RHF}|\Phi_j^b\rangle|t\rangle &= (\varepsilon_a - \varepsilon_i + d_c + \tilde{\omega}\, t)\delta_{ij}\delta_{ab}\delta_{st} + \delta_{st}(2(ia|jb) - (ij|ab)) + 2\delta_{st}\sum_{\xi,\xi'}\lambda^\xi\lambda^{\xi'}\mu_{ia}^\xi\mu_{jb}^\xi - \delta_{st}\sum_{\xi,\xi'}\lambda^\xi\lambda^{\xi'}\mu_{ij}^\xi\mu_{ab}^\xi \\ &+ \sqrt{t+1}\,\delta_{s,t+1}\delta_{ij}\delta_{ab}\sqrt{\frac{\tilde{\omega}}{2}}\lambda\cdot\langle\mu\rangle + \sqrt{t}\,\delta_{s,t-1}\delta_{ij}\delta_{ab}\sqrt{\frac{\tilde{\omega}}{2}}\lambda\cdot\langle\mu\rangle - \sqrt{t+1}\,\delta_{s,t+1}\delta_{ij}\delta_{ab}\sqrt{\frac{\tilde{\omega}}{2}}\sum_\xi\sum_k\lambda^\xi\mu_{kk}^\xi \\ &- \sqrt{t}\,\delta_{s,t-1}\delta_{ij}\delta_{ab}\sqrt{\frac{\tilde{\omega}}{2}}\sum_\xi\sum_k\lambda^\xi\mu_{kk}^\xi - \sqrt{t+1}\,\delta_{s,t+1}\delta_{ij}\sqrt{\frac{\tilde{\omega}}{2}}\sum_\xi\lambda^\xi\mu_{ab}^\xi - \sqrt{t}\,\delta_{s,t-1}\delta_{ij}\sqrt{\frac{\tilde{\omega}}{2}}\sum_\xi\lambda^\xi\mu_{ab}^\xi \\ &+ \sqrt{t+1}\,\delta_{s,t+1}\delta_{ab}\sqrt{\frac{\tilde{\omega}}{2}}\sum_\xi\lambda^\xi\mu_{ij}^\xi + \sqrt{t}\,\delta_{s,t-1}\delta_{ab}\sqrt{\frac{\tilde{\omega}}{2}}\sum_\xi\lambda^\xi\mu_{ij}^\xi.\end{aligned} \tag{9}$$

Since this NH-CQED-CIS Hamiltonian is non-Hermitian, the left and right eigenvectors, which we will denote as Ψ_I^L and Ψ_I^R for the left and right eigenvectors for the NH-CQED-CIS state I, respectively, are not simply complex conjugates of each other. However, the left and right eigenvectors can be chosen to be biorthogonal, where biorthogonality implies that[45]

$$\langle\Psi_I^L|\Psi_J^R\rangle = \delta_{IJ}. \tag{10}$$

Using a biorthogonal basis enables one to compute the expectation values for a given state I (e.g., the energy or dipole moment) or the transition values between states I and J (e.g., the transition dipole moment) using the left and right eigenvectors as the bra and ket states,[45]

$$\langle O_I\rangle = \langle\Psi_I^L|\hat{O}|\Psi_I^R\rangle \tag{11}$$

and

$$\langle O_{IJ}\rangle = \langle\Psi_I^L|\hat{O}|\Psi_J^R\rangle. \tag{12}$$

In our reference implementation, we enforce biorthogonality by using a scheme based on LU decomposition.

TABLE I. Change in total CQED-RHF energy (ΔE in eV) and percentage relative changes in different contributions to the total CQED-RHF energy for three different polarizations of a photonic mode with magnitude $|\lambda| = 0.1$ a.u. The terms Δ_{1E} and Δ_{2E} denote the changes in the RHF one- and two-electron energies, respectively, and the terms Δ_{1de}, Δ_{2de}, Δ_{1qe}, and Δ_{d_c} denote changes in the CQED-RHF one-electron dipole, two-electron dipole, one-electron quadrupole, and dipole constant terms, respectively.

Total	Canonical RHF		Cavity contributions			
ΔE (eV)	% Δ_{1E}	% Δ_{2E}	% Δ_{1de}	% Δ_{1qe}	% Δ_{2de}	% Δ_{d_c}
			λ_y			
0.925	−229	230	0	209	−110	0
			λ_z			
1.110	−178	179	−31	431	−316	15
			λ_{yz}			
1.034	−200	201	−16	329	−222	8

© Author(s) 2022

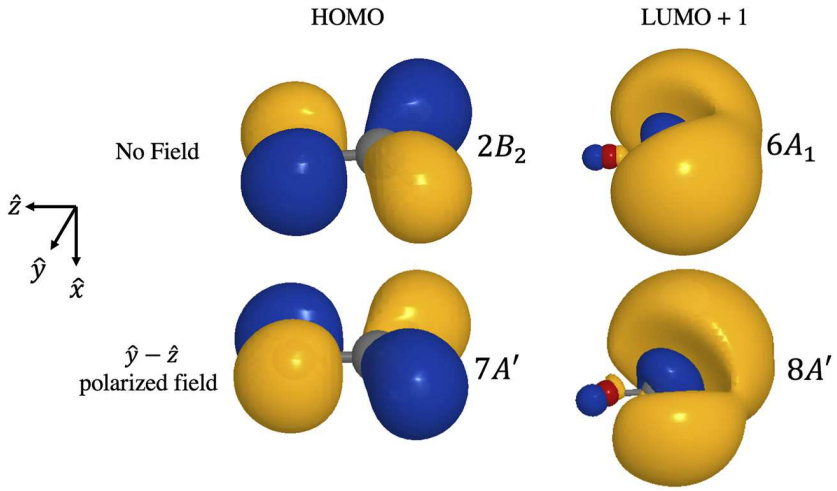

FIG. 1. Comparison of the HOMO and LUMO+1 orbitals of formaldehyde uncoupled to a photon mode (top) and strongly coupled to a photon mode polarized along the *y*–*z* axis (bottom), where strong coupling results in a change in symmetry from C_{2v} to C_s.

III. REFERENCE IMPLEMENTATIONS

We provide reference implementations by using Psi4Numpy,[44] which provides a simple NumPy interface to the Psi4[46] quantum chemistry engine. The code for these reference implementations can be freely accessed in the hilbert package[47] and the Psi4Numpy project.[48] Furthermore, to provide a no-installation option for interested users to experiment with these implementations, we utilize the ChemCompute project[49] to host the illustrative calculations discussed in Sec. IV. Interested users can navigate to https://chemcompute.org/register to register for a free ChemCompute account. Following the registration, interested users can run calculations described in Table I in Sec. IV using the link within Ref. 50, the calculations described in Fig. 1 using the link within Ref. 51, the results described in Table II and Fig. 2 using the link in Ref. 52, the results illustrated in Fig. 3 using the link within Ref. 53, the results illustrated in Fig. 4 using the link within Ref. 54, and the results in Figs. 5 and 6 in Appendixes A–C using the link within Ref. 55.

IV. RESULTS

We apply the CQED-RHF and NH-CQED-CIS approaches to a few simple polaritonic chemical systems. First, we examine the ground-state of formaldehyde strongly coupled to a single photon mode, which has been explored by several groups that have been developing density functional theory-based *ab initio*-QED methods.[11,38] We optimize the geometry of lone formaldehyde at the RHF/cc-pVDZ level and perform all calculations at that geometry (see Ref. 50). At this level, the RHF ground-state has a dipole moment oriented purely along the z axis with $\langle\mu\rangle_z = -1.009$ a.u. The CQED-RHF equations are solved for a fixed magnitude of the coupling vector $|\lambda| = 0.1$ a.u. with the following three polarizations: $\lambda_y = (0, |\lambda|, 0)$, $\lambda_z = (0, 0, |\lambda|)$, and $\lambda_{yz} = \left(0, \frac{|\lambda|}{\sqrt{2}}, \frac{|\lambda|}{\sqrt{2}}\right)$. This value of λ is quite large and leads to a coupling energy scale $\hbar g \approx \hbar\sqrt{\frac{\omega}{2}}\lambda\mu \approx 1$ eV, which is ~10 times larger than the single molecule coupling strength reported by Chikkaraddy *et al.*[4] However, as in Ref. 31, where the same coupling magnitude was considered to illustrate cavity modifications to intermolecular interactions, we note that such coupling strengths could be conceivable considering that experimental cavities will have many modes and the effective coupling arises as the norm of all the mode coupling parameters.

The ground-state energy, as predicted by the CQED-RHF method, departs from the RHF energy in all three cases, with the largest deviation coming from λ_z case (see Table I), which would be expected, given that the permanent dipole moment is oriented along the z axis. However, the deviations seen by the λ_y and λ_{yz} cases point to subtle effects arising from the quadrupolar terms in the quadratic self-energy and the two-electron contribution to the quadratic self-energy. To quantify these various contributions, we look at the changes in the various contributions to the CQED-RHF energy with and without coupling to the photon field. For example, we define the change in the canonical RHF one-electron energy resulting from the photon field in the λ_{yz} case as

$$\Delta_{1E} = \sum_{\mu\nu} 2h_{\mu\nu}D_{\mu\nu}^{\lambda_{yz}} - 2h_{\mu\nu}D_{\mu\nu}, \tag{13}$$

where $D_{\mu\nu}^{\lambda_{yz}}$ are the elements of the converged CQED-RHF density matrix in the λ_{yz} case and $D_{\mu\nu}$ are the elements of the CQED-RHF density matrix in the absence of coupling to a photon (i.e., the canonical RHF density matrix). We tabulate the changes in these various CQED-RHF contributions for the λ_z, λ_y, and λ_{yz} cases in Table I.

TABLE II. Changes in the ground-state energy predicted by the NH-CQED-CIS method relative to the canonical RHF energy as well as the CQED-RHF energy in atomic units. Calculations were performed with a fixed magnitude of $|\lambda| = 0.1$ a.u. for the λ_z and λ_{yz} polarizations. NH-CQED-CIS method calculations were performed to reflect formaldehyde coupling to a photon with $\hbar\omega = 10.4$ eV.

	Relative to RHF	Relative to CQED-RHF
Polarization	ΔE (eV)	ΔE (eV)
λ_z	0.811	−0.318
λ_{yz}	0.771	−0.266

© Author(s) 2022

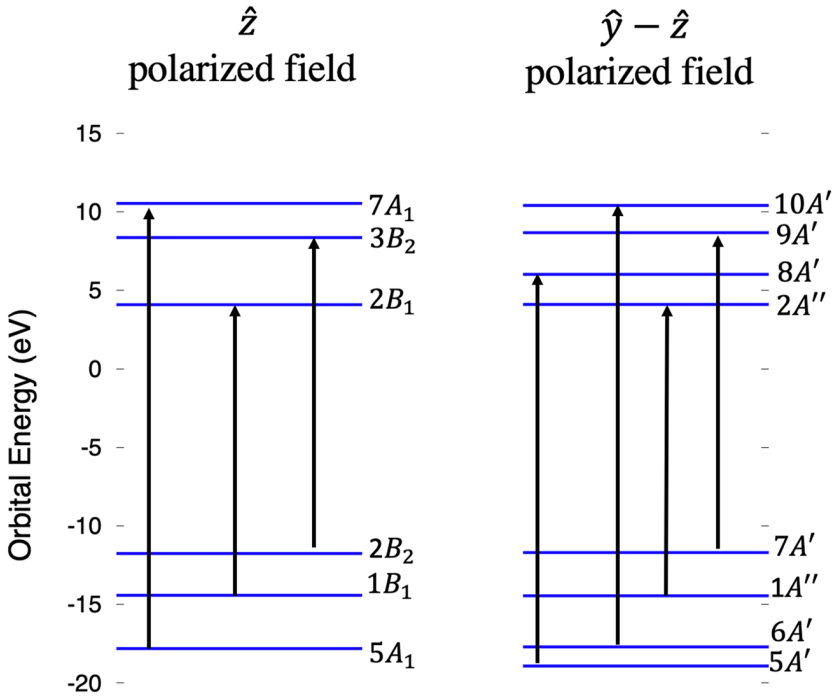

FIG. 2. Dominant single excitations from the CQED-RHF reference that contribute to the NH-CQED-CIS ground-state wavefunction when formaldehyde is coupled to a photon with $\omega = 0.382$ a.u. ($\hbar\omega = 10.4$ eV) polarized along the z axis with $\lambda_z = 0.1$ a.u. (left) and $y - z$ axis (right) with $\lambda_y = \lambda_z = 0.1/\sqrt{2}$ a.u. (right).

The one-electron quadrupolar and two-electron dipolar terms that arise from $\hat{H}_{dse}$ typically comprise the largest changes to the CQED-RHF energy from the three polarizations considered in Table I. However, the changes in the canonical RHF one- and two-electron terms (denoted by Δ_{1E} and Δ_{2E}) suggest that changes to the ground-state electron density via the CQED-RHF orbitals arise from coupling to the cavity modes. Although these changes largely cancel each other in the total energy (i.e., $\Delta_{1E} \approx -\Delta_{2E}$ in all three cases), it is, nevertheless, interesting to view the impact of cavity coupling on the CQED-RHF orbitals. The RHF orbitals for the HOMO ($2B_2$) and LUMO+1 ($6A_1$) of formaldehyde uncoupled to a photon are compared to their corresponding CQED-RHF orbitals for the λ_{yz} case ($7A'$ and $8A'$), where the orbitals are noticeably distorted (see Fig. 1). The reshaping of the CQED-RHF orbitals in the λ_{yz} case results in a loss of symmetry from C_{2v} to C_s and impacts both ground-state energy and properties. As seen in Table I, there is no one-electron dipole contribution to the energy shift in the λ_y case since the ground-state dipole moment is oriented purely along the z axis. However, in the λ_{yz} case, the distortion of the ground-state orbitals results in a reorientation of the dipole moment to point along the yz axis with value $\langle\mu\rangle = (0, -0.025, -1.16)$ a.u. We see that this reorientation of the ground-state dipole moment is accompanied by the changes in the ground-state energy specifically attributable to the one-electron dipolar terms, CQED-RHF Fock operator (see Table I). In principle, this change in ground-state dipole moment could be experimentally confirmed through rotational spectroscopy. In particular, because the oscillator strength of a given transition involves integrals over the dipole moment $f \propto |\int_0^{2\pi}\int_0^{\pi} d\phi d\theta \psi_i(\theta,\phi)\hat{\mu}(\theta,\phi)\psi_f(\theta,\phi)|^2$, and the dipole moment in the cavity-coupled case takes on an orientation dependence compared to the lone molecular case, the oscillator strengths in the cavity case would be modified in turn.

Turning to the NH-CQED-CIS Hamiltonian, it can be seen that, unlike the canonical CIS method, the NH-CQED-CIS method couples single excitations of the electronic and photonic terms to the CQED-RHF reference state. Specifically, it can be seen in Eq. (8) that the CQED-RHF wavefunction can couple to states that involve singly excited electronic configurations and singly occupied photon states. This coupling can lower the energy of the lowest energy eigenstate of the NH-CQED-CIS Hamiltonian relative to the ground-state determined by the CQED-RHF method (see Table II). The cavity-induced modification to the symmetry of the CQED-RHF wavefunction has important consequences for which singly excited configurations can contribute to the ground-state. We examine the impacts of this cavity effect again with formaldehyde coupled to a lossless photon with $\omega = 0.382$ a.u. (10.4 eV), which is approximately resonant with the first two dipole allowed transitions at the CIS/cc-pVDZ level of theory (see Ref. 52). We consider the same coupling magnitudes as before, this time focusing only on the λ_z and λ_{yz} cases. The polarization vector in the λ_z case belongs to the A_1 irrep of the C_{2v} point group, while the polarization vector in the λ_{yz} case belongs to the A' irrep of the C_s point group. In Fig. 2, we present the dominant singly excited contributions to the NH-CQED-CIS ground-state in the λ_z and λ_{yz} cases. We, indeed, see a slightly more permissive mixing of singly excited configurations into the NH-CQED-CIS ground-state in the λ_{yz} case due to the lower symmetry of the wavefunction. We report the changes in the ground-state energy as predicted by the NH-CQED-CIS method relative to the canonical RHF method and the CQED-RHF method in Table II.

© Author(s) 2022

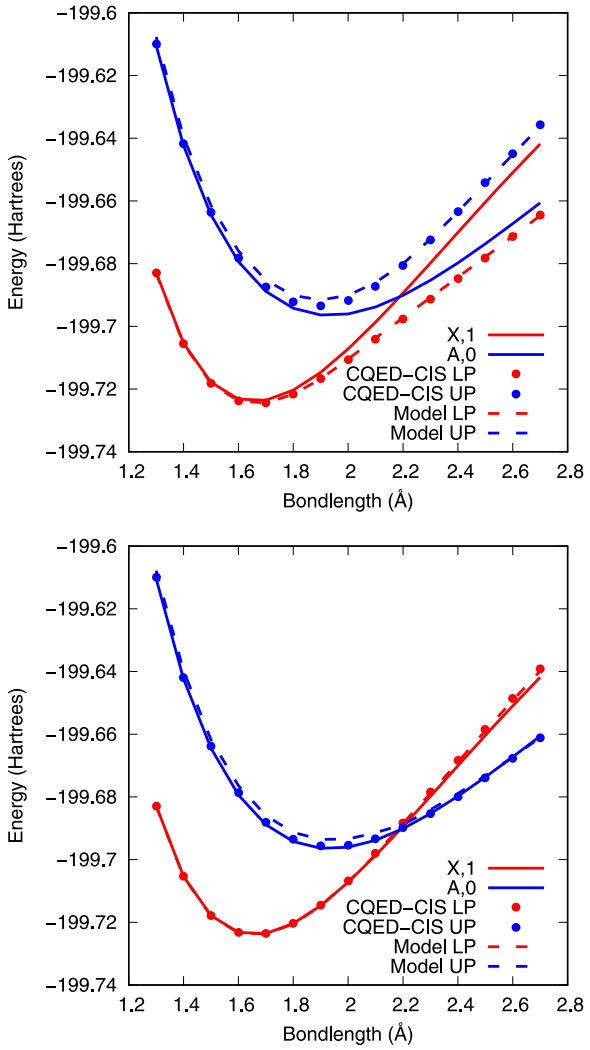

FIG. 3. Polaritonic surface of MgH+ coupled to a photon with (top) $\hbar\tilde{\omega} = 4.75$ eV and (bottom) $\hbar\tilde{\omega} = 4.75–0.45i$ eV with $\lambda_z = 0.0125$ a.u. We see evidence of strong coupling via splitting of the surfaces where the $|X,1\rangle$ and $|A,0\rangle$ states are resonant when the photon energy is purely real, and we see the splitting vanish when the imaginary part of the photon energy is large compared to the interaction energy.

As a second illustrative example of the NH-CQED-CIS method, we consider the upper-polariton ($|UP\rangle$) and lower-polariton ($|LP\rangle$) states that emerge from coupling MgH^+ to a photon resonant with the ground-state to first singlet excited-state ($|X\rangle \rightarrow |A\rangle$) transition.[25] We consider the photon to be polarized along the z axis, in alignment with the relevant transition dipole moment, with $\lambda_z = 0.0125$ a.u. This time, we allow the photon to have complex energy where the imaginary part accounts for photonic dissipation, which can also be related to the energy uncertainty of the photonic mode.[27] We consider the real part of the photon energy to be 4.75 eV and the imaginary part to be either 0 eV or 0.45 eV. This value of λ leads to a coupling energy scale $\hbar g \approx \hbar\sqrt{\frac{\omega}{2}}\lambda\mu \approx 0.1$ eV, which is comparable to the single molecule coupling strength reported

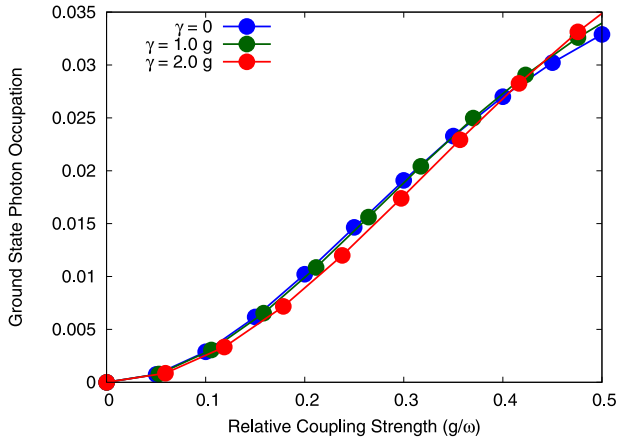

FIG. 4. Approximate photon occupations of the NH-CQED-CIS/cc-pVDZ ground-state of MgH+ at a bondlength of 2.2 Å as a function of the relative coupling energy scale, $g/\mathrm{Re}(\tilde{\omega})$, and the dissipation energy scale γ. In this case, $g \approx \sqrt{\frac{\omega}{2}}\lambda_z\mu_z$ for MgH+, where $\lambda_z = 0.0125$ a.u., $\mathrm{Re}(\hbar\tilde{\omega}) = 4.75$ eV. We see the approximate quadratic scaling of the photon occupation with the relative coupling strength in the ground-state at all loss rates, in agreement with the analytical findings discussed in Ref. 6.

by Chikkaraddy *et al.*[4] Similarly, the dissipation energy scale of 0.45 eV corresponds to approximately a 10 fs lifetime, which is shorter but on a similar order to the lifetimes of the plasmonic resonances reported in Ref. 4. We specifically chose this value because it represents the $\gamma = 4g$ threshold at which the Rabi splitting of polaritonic surfaces associated with strong coupling disappears.[6,27] For context to the lifetime of the plasmonic cavities in Ref. 4, one can infer photonic lifetimes from the scattering linewidth of their bare plasmonic cavity setup, which are ~115 meV, suggesting a lifetime of around 38 fs.

The two lowest-lying excited-states of NH-CQED-CIS with both photon frequency values are plotted as a function of the bondlength for values between 1.3 and 2.7 Å with increments of 0.1

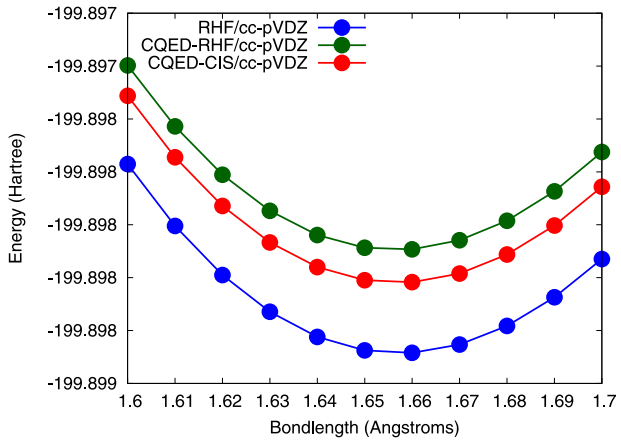

FIG. 5. Potential energy surface of the ground-state of MgH+ as computed by the RHF/cc-pVDZ, CQED-RHF/cc-pVDZ, and NH-CQED-CIS/cc-pVDZ methods.

© Author(s) 2022

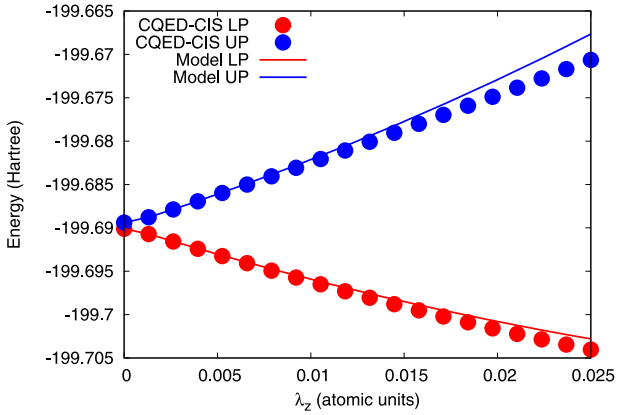

FIG. 6. Comparison of eigenvalues of the lower- and upper-polariton states as computed by the NH-CQED-CIS/cc-pVDZ method and the model Hamiltonian in Eq. (14) parameterized by CIS/cc-pVDZ methods for MgH+ with a bondlength of 2.2 Å coupled to a photon with energy 4.75 eV at variable coupling strengths.

Å (see Ref. 53) in Fig. 3. In addition to computing these polariton surfaces at the NH-CQED-CIS/cc-pVDZ level, we compute these polaritonic surfaces at the same values of the MgH+ bondlength R using a model three-level Hamiltonian,

$$\mathrm{H} = \begin{pmatrix} E_X + \frac{(\lambda \cdot \langle \mu_X \rangle)^2}{2} & 0 & 0 \\ 0 & E_X + \tilde{\omega} + \frac{(\lambda \cdot \langle \mu_X \rangle)^2}{2} & \sqrt{\frac{\tilde{\omega}}{2}} \lambda \cdot \mu_{XA} \\ 0 & \sqrt{\frac{\tilde{\omega}}{2}} \lambda \cdot \mu_{XA} & E_A + \frac{(\lambda \cdot \langle \mu_A \rangle)^2}{2} \end{pmatrix}, \tag{14}$$

where E_X ($\langle \mu_X \rangle$) and E_A ($\langle \mu_A \rangle$) denote the ground-state and first singlet excited-state energies (dipole moments), respectively, and μ_{XA} denotes the transition dipole moment between states X and A. The ground-state energies and dipole moments for each value of R are calculated at the RHF/cc-pVDZ level, and the excited-state energies, dipole moments, and transition dipole moments are calculated at the CIS/cc-pVDZ level (see Ref. 53). The polaritonic surfaces obtained from diagonalizing Eq. (A8) are referred to as the "Model LP" and "Model UP" surfaces in Fig. 3. We see with a pure real photon energy, the $|LP\rangle$ and $|UP\rangle$ surfaces experience a strong splitting in the region where the $|X, 1\rangle$ state (the ground-state plus a photon) crosses the $|A, 0\rangle$ state (the first excited-state without a photon). It should be noted that the NH-CQED-CIS curves are typically slightly stabilized compared to the Model LP and UP curves. We have already seen that the CQED-RHF method can provide orbital relaxation in the presence of cavity coupling that would not be available to the Model LP and UP solutions, and the NH-CQED-CIS wavefunction also includes additional variational flexibility through the excitations coupled through the $\hat{H}_{dse}$ and $\hat{H}_{ep}$ terms. It is interesting to consider when such deviations between the NH-CQED-CIS and simpler model Hamiltonians arise; we explore this question with the MgH+ system as a function of fundamental coupling strength λ in Appendix C. For a strongly dissipative photon, we see that both the model and CQED-CIS curves closely approximate the CIS curves for the lone molecules, which signals that this system is not in the strong-coupling regime. The loss of strong coupling, in this case, arises because the dissipative energy scale of the photon is significant compared to the interaction energy scale between the photon and the molecular transition.[27] This echos a fundamental condition for strong coupling that the interaction strength $\hbar g$ must be large compared to the dissipation energy scale $\hbar\gamma$, specifically $\hbar g > \hbar\frac{\gamma}{4}$. If this condition is not satisfied, then the energy splitting between the interacting states vanishes. The imaginary part of the frequency giving rise to the curves shown in the bottom panel of Fig. 3 was specifically chosen so that $\hbar g < \hbar\frac{\gamma}{4}$, leading to the vanishing of the splitting that is observed in the top panel of Fig. 3.

As a final illustrative example, we examine the approximate ground-state photon population of the MgH+ system for coupling strengths approaching the ultra-strong coupling regime, defined when the coupling energy scale is commensurate with the bare excitations in the system, e.g., $g \approx \mathrm{Re}(\tilde{\omega})$. We approximate the ground-state photon occupation as $N_p = |c_0^1|^2 + \sum_{ia} |c_{ia}^1|^2$, where the c coefficients are taken from the lowest root of the NH-CQED-CIS Hamiltonian matrix. We see an approximate quadratic dependence of the photon occupation in the ground-state as a function of relative coupling strengths independent of the dissipation energy scale (see Fig. 4). The results of this analysis agree qualitatively with the analytical analysis of the ground-state populations of the ground-state wavefunctions of dissipative systems in the ultra-strong coupling regime by De Liberato.[6] An important point raised by this work is that features associated with the ultra-strong coupling regime (e.g., virtual photon occupation in the ground-state) persist even in the presence of very strong dissipation that would obscure the effects normally associated with strong-coupling (e.g., Rabi splitting).[6] Similar to our analysis illustrated in Fig. 4, the exact analysis also showed photon occupation of the ground-state wavefunction increases quadratically with the relative coupling strength, where the relative coupling strength is defined as $g/\mathrm{Re}(\tilde{\omega})$, where g relates to the coupling energy scale. To determine if our NH-CQED-CIS obeys this scaling relationship for the photon occupation of the ground-state, we compute the photon occupations for the ground-state of MgH+ computed at the NH-CQED-CIS/cc-pVDZ level of theory with bondlength fixed at r = 2.2 Å for relative coupling strengths $g/\mathrm{Re}(\tilde{\omega})$ in a range of values between 0 and 0.5, where in our case $g \approx \sqrt{\frac{\tilde{\omega}}{2}} \lambda_z \mu_z$ and $\mathrm{Re}(\hbar\tilde{\omega})$ = 4.75 eV throughout (resonant with the $|X\rangle \rightarrow |A\rangle$)transition at this geometry, λ_z = 0.0125 a.u., $\lambda_z \approx$ 2.2 a.u., and $\mathrm{Im}(\hbar\tilde{\omega})$ is chosen relative to g. We emphasize that this qualitative analysis involves coupling strengths that are much larger than those realized in any experiments we are aware of with molecular systems, and serve purely to analyze the behavior of our approximate NH-CQED-CIS method compared to the exact analysis provided in Ref. 6.

V. CONCLUSIONS

We combined *ab initio* molecular electronic Hamiltonians with a cavity quantum electrodynamics model for dissipative photonic modes and applied mean-field theories to the ground- and excited-states of resulting polaritonic systems. In particular, we developed a non-Hermitian configuration interaction singles theory for mean-field ground- and excited-states of the molecular system strongly interacting with a photonic mode, and we applied these methods

© Author(s) 2022

with the purpose of elucidating the phenomenology of paradigmatic polaritonic systems, including the ground-state polaritonic structure of formaldehyde coupled to cavity modes that were shown to modify the symmetry of the ground-state wavefunction and the polaritonic potential energy surfaces of the magnesium hydride ion coupled to a lossy photonic mode. A reference implementation of this method and the CQED-RHF method was realized by using the Psi4Numpy framework that can be accessed using links provided within the text.

ACKNOWLEDGMENTS

J.M. and J.J.F. acknowledge the support from the Research Corporation for Scientific Advancement Cottrell Scholar Award and the NSF CAREER Award (Grant No. CHE-2043215). Computational resources were provided, in part, by the MERCURY consortium (http://mercuryconsortium.org/) under the NSF (Grant Nos. CHE-1229354, CHE-1662030, and CHE-2018427). We thank A. E. DePrince III for numerous helpful discussions and access to benchmark results for the CQED-RHF method.

AUTHOR DECLARATIONS

Conflict of Interest

The authors have no conflicts to disclose.

DATA AVAILABILITY

The data that support the findings of this study are available from the corresponding author upon reasonable request and are openly available in GitHub at https://github.com/FoleyLab/psi4polaritonic.[50–55]

APPENDIX A: CQED-RHF THEORY

The orbital basis and reference determinant utilized in the NH-CQED-CIS theory result from solving the CQED-RHF equations. We start with a Hermitian version of Eq. (1) that utilizes a pure real value of $\tilde{\omega}$, and following Refs. 26 and 29, we introduce a product wavefunction between an electronic Slater determinant (which, in practice, may be initialized using a canonical RHF wavefunction) and a zero-photon number state,

$$|R\rangle = |\Phi_0\rangle|0\rangle. \tag{A1}$$

To develop CQED-RHF theory, we examine the expectation value of Eq. (1) with respect to Eq. (A1),

$$\begin{aligned}\langle R|\hat{H}_{ep}|R\rangle + \langle 0|\hat{H}_p|0\rangle + \langle\Phi_0|\hat{H}_e + \hat{H}_{dse}|\Phi_0\rangle \\ = \langle\Phi_0|\hat{H}_e|\Phi_0\rangle + \langle\Phi_0|\hat{H}_{dse}|\Phi_0\rangle,\end{aligned} \tag{A2}$$

where we see that the terms involving $\hat{H}_p$ and $\hat{H}_{ep}$ vanish and the expectation value of $\hat{H}_e$ is analogous to the ordinary RHF energy. To evaluate the expectation value of $\hat{H}_{dse}$, we can first expand $\hat{H}_{dse}$ in terms of the dipole operator (with electronic and nuclear contributions) and dipole expectation values as follows:

$$\begin{aligned}\hat{H}_{dse} = &\sum_{\xi,\xi'}\sum_{i,j>i}\lambda^\xi\lambda^{\xi'}\hat{\mu}^\xi(x_i)\hat{\mu}^{\xi'}(x_j) - \frac{1}{2}\sum_{\xi,\xi'}\sum_i\lambda^\xi\lambda^{\xi'}\hat{Q}^{\xi\xi'}(x_i) \\ &+ (\lambda\cdot\mu_{nuc} - \lambda\cdot\langle\mu\rangle)\sum_\xi\sum_i\lambda^\xi\hat{\mu}^\xi(x_i) \\ &+ \frac{1}{2}(\lambda\cdot\mu_{nuc})^2 - (\lambda\cdot\langle\mu\rangle)(\lambda\cdot\mu_{nuc}) + \frac{1}{2}(\lambda\cdot\langle\mu\rangle)^2.\end{aligned} \tag{A3}$$

In the above expansion of $\hat{H}_{dse}$, we have specifically indicated that the product of electronic dipole operators contains two-electron contributions when $i \neq j$ and one-electron quadrupole contributions when $i = j$. The quadrupole contributions arise from the fact that $\hat{\mu}^\xi(x_i)\hat{\mu}^{\xi'}(x_i) = -\hat{Q}^{\xi\xi'}(x_i)$. Furthermore, a one-electron term arises that contains the electronic dipole operator scaled by $\lambda\cdot\mu_{nuc} - \lambda\cdot\langle\mu\rangle$, where again $\langle\mu\rangle$ will be iteratively updated during the CQED-RHF procedure.

To solve the CQED-RHF equations, the additional one-electron terms above will be added to the typical core Hamiltonian elements $h_{\mu\nu}$ that arises in canonical Hartree–Fock theory, and the additional two-electron terms above will be included in the density-matrix dependent terms in the Fock operator,

$$F_{\mu\nu} = H_{\mu\nu} + G_{\mu\nu}, \tag{A4}$$

where

$$H_{\mu\nu} = h_{\mu\nu} - \frac{1}{2}\sum_{\xi,\xi'}\lambda^\xi\lambda^{\xi'}Q^{\xi\xi'}_{\mu\nu} + (\lambda\cdot\mu_{nuc} - \lambda\cdot\langle\mu\rangle)\sum_\xi\lambda^\xi\mu^\xi_{\mu\nu} \tag{A5}$$

and

$$\begin{aligned}G_{\mu\nu} = &(2(\mu\,\nu|\,\lambda\,\sigma) - (\mu\,\lambda\,|\nu\,\sigma))D_{\lambda\sigma} \\ &+ \left(\sum_{\xi\xi'}\lambda^\xi\lambda^{\xi'}\left(2\,\mu^\xi_{\mu\nu}\mu^{\xi'}_{\lambda\sigma} - \mu^\xi_{\mu\lambda}\mu^{\xi'}_{\nu\sigma}\right)\right)D_{\lambda\sigma},\end{aligned} \tag{A6}$$

leading to the total QED-RHF energy being

$$E_{CQED-RHF} = (F_{\mu\nu} + H_{\mu\nu})D_{\mu\nu} + V_{NN} + d_c, \tag{A7}$$

where

$$d_c = \frac{1}{2}(\lambda\cdot\mu_{nuc})^2 - (\lambda\cdot\langle\mu\rangle)(\lambda\cdot\mu_{nuc}) + \frac{1}{2}(\lambda\cdot\langle\mu\rangle)^2. \tag{A8}$$

For clarity, we briefly outline the CQED-RHF algorithm as follows:

1. Compute kinetic, nuclear attraction, electron repulsion, dipole, and quadrupole integrals in AO basis.
2. Perform canonical RHF calculation.
3. Initialize **D** and $\langle\mu\rangle$ from canonical RHF wavefunction.
4. Augment core Hamiltonian with the dipole and quadrupole terms in Eq. (A5).
5. Augment the Fock matrix by contracting products of dipole integrals over current density matrix in Eq. (A6).
6. Compute SCF energy through Eq. (A7).
7. Diagonalize Fock matrix and update density matrix.
8. Check for convergence; if not converged, return to step 5.

© Author(s) 2022

APPENDIX B: MODIFICATION OF MOLECULAR GEOMETRY UNDER STRONG COUPLING

Given the modifications to the polaritonic potential energy surfaces observed in Fig. 3 in the main text, it is interesting to consider if the ground-state potential energy surfaces can also be modified. While such modifications would be discernible from ground-state *ab initio* polaritonic structure methods, we suspect the onset would not be observed until the onset of ultra-strong coupling and perhaps still under special conditions like the field polarization being oriented relative to a permanent dipole moment in particular ways. Here, we consider only the case of the equilibrium geometry of the ground-state of MgH+ computed at the RHF/cc-pVDZ, CQED-RHF/cc-pVDZ, and CQED-CIS/cc-pVDZ levels of theory with the same coupling parameters considered in the main text for this system, namely, $\hbar\omega = 4.75$ eV and $\lambda = (0, 0, 0.0125)$ a.u. The potential energy curves from each of these methods are shown in Fig. 5, and we find from the numerical location of the minima that the equilibrium bondlength predicted by all levels of theory is ~1.65 Å.

APPENDIX C: ONSET OF DEVIATIONS BETWEEN ATOMISTIC AND MODEL POLARITONIC STATES

In Fig. 3, we see deviations between the polaritonic surfaces computed by the NH-CQED-CIS/cc-pVDZ method and those computed by a simpler 3×3 model Hamiltonian that is parameterized by CIS/cc-pVDZ calculations of MgH+. In Fig. 6, we explore the eigenvalues of these two approaches for the lower- and upper-polariton surfaces of MgH+ with bondlength fixed at 2.2 Å coupled to a photon with energy 4.75 eV with variable values of λ_z between 0 and 0.025 a.u., which is approximately twice the value considered in Fig. 3. We see that deviations between the model Hamiltonian and the NH-CQED-CIS results become evident when the fundamental coupling strength λ has a magnitude between 0.01 and 0.015 a.u., which is in the range of values we considered for Fig. 3, and that is also in line with experimentally realized coupling strengths reported in Ref. 4.

REFERENCES

[1] J. A. Hutchison, T. Schwartz, C. Genet, E. Devaux, and T. W. Ebbesen, "Modifying chemical landscapes by coupling to vacuum fields," Angew. Chem., Int. Ed. **51**, 1592–1596 (2012).

[2] J. Galego, F. J. Garcia-Vidal, and J. Feist, "Cavity-induced modifications of molecular structure in the strong-coupling regime," Phys. Rev. X **5**, 041022 (2015).

[3] T. W. Ebbesen, "Hybrid light-matter states in a molecular and material science perspective," Acc. Chem. Res. **49**, 2403–2412 (2016).

[4] R. Chikkaraddy, B. de Nijs, F. Benz, S. J. Barrow, O. A. Scherman, E. Rosta, A. Demetriadou, P. Fox, O. Hess, and J. J. Baumberg, "Single-molecule strong coupling at room temperature in plasmonic nanocavities," Nature **535**, 127–130 (2016).

[5] F. Herrera and F. C. Spano, "Cavity-controlled chemistry in molecular ensembles," Phys. Rev. Lett. **116**, 238301 (2016).

[6] S. De Liberato, "Virtual photons in the ground state of a dissipative system," Nat. Commun. **8**, 1465 (2017).

[7] N. M. Hoffmann, H. Appel, A. Rubio, and N. T. Maitra, "Light-matter interactions via the exact factorization approach," Eur. Phys. J. B **91**, 180 (2018).

[8] J. Feist, J. Galego, and F. J. Garcia-Vidal, "Polaritonic chemistry with organic molecules," ACS Photonics **5**, 205–216 (2018).

[9] L. A. Martínez-Martínez, R. F. Ribeiro, J. Campos-González-Angulo, and J. Yuen-Zhou, "Can ultrastrong coupling change ground-state chemical reactions?," ACS Photonics **5**, 167–176 (2018).

[10] B. Munkhbat, M. Wersäll, D. G. Baranov, T. J. Antosiewicz, and T. Shegai, "Suppression of photo-oxidation of organic chromophores by strong coupling to plasmonic nanoantennas," Sci. Adv. **4**, eaas9552 (2018).

[11] J. Flick and P. Narang, "Cavity-correlated electron-nuclear dynamics from first principles," Phys. Rev. Lett. **121**, 113002 (2018).

[12] J. Fregoni, G. Granucci, E. Coccia, M. Persico, and S. Corni, "Manipulating azobenzene photoisomerization through strong light-molecule coupling," Nat. Commun. **9**, 4688 (2018).

[13] L. A. Martínez-Martínez, M. Du, R. F. Ribeiro, S. Kéna-Cohen, and J. Yuen-Zhou, "Polariton-assisted singlet fission in acene aggregates," J. Phys. Chem. Lett. **9**, 1951–1957 (2018).

[14] L. A. Martínez-Martínez, E. Eizner, S. Kéna-Cohen, and J. Yuen-Zhou, "Triplet harvesting in the polaritonic regime: A variational polaron approach," J. Chem. Phys. **151**, 054106 (2019).

[15] O. Di Stefano, A. Settineri, V. Macrì, L. Garziano, R. Stassi, S. Savasta, and F. Nori, "Resolution of gauge ambiguities in ultrastrong-coupling cavity quantum electrodynamics," Nat. Phys. **15**, 803–808 (2019).

[16] M. Du, R. F. Ribeiro, and J. Yuen-Zhou, "Remote control of chemistry in optical devices," Chem **5**, 1167–1181 (2019).

[17] A. Mandal and P. Huo, "Investigating new reactivities enabled by polariton photochemistry," J. Phys. Chem. Lett. **10**, 5519–5529 (2019).

[18] A. Mandal, T. D. Krauss, and P. Huo, "Polariton-mediated electron transfer via cavity quantum electrodynamics," J. Phys. Chem. B **124**, 6321–6340 (2020).

[19] M. A. D. Taylor, A. Mandal, W. Zhou, and P. Huo, "Resolution of gauge ambiguities in molecular cavity quantum electrodynamics," Phys. Rev. Lett. **125**, 123602 (2020).

[20] S. Felicetti, J. Fregoni, T. Schnappinger, S. Reiter, R. de Vivie-Riedle, and J. Feist, "Photoprotecting uracil by coupling with lossy nanocavities," J. Phys. Chem. Lett. **11**, 8810 (2020).

[21] J. Fregoni, S. Corni, M. Persico, and G. Granucci, "Photochemistry in the strong coupling regime: A trajectory surface hopping scheme," J. Comput. Chem. **41**, 2033–2044 (2020).

[22] J. Fregoni, G. Granucci, M. Persico, and S. Corni, "Strong coupling with light enhances the photoisomerization quantum yield of azobenzene," Chem **6**, 250–265 (2020).

[23] I. S. Ulusoy and O. Vendrell, "Dynamics and spectroscopy of molecular ensembles in a lossy microcavity," J. Chem. Phys. **153**, 044108 (2020).

[24] N. M. Hoffmann, L. Lacombe, A. Rubio, and N. T. Maitra, "Effect of many modes on self-polarization and photochemical suppression in cavities," J. Chem. Phys. **153**, 104103 (2020).

[25] E. Davidsson and M. Kowalewski, "Simulating photodissociation reactions in bad cavities with the lindblad equation," J. Chem. Phys. **153**, 234304 (2020).

[26] T. S. Haugland, E. Ronca, E. F. Kjønstad, A. Rubio, and H. Koch, "Coupled cluster theory for molecular polaritons: Changing ground and excited states," Phys. Rev. X **10**, 041043 (2020).

[27] P. Antoniou, F. Suchanek, J. F. Varner, and J. J. Foley IV, "Role of cavity losses on nonadiabatic couplings and dynamics in polaritonic chemistry," J. Phys. Chem. Lett. **11**, 9063–9069 (2020).

[28] M. H. Farag, A. Mandal, and P. Huo, "Polariton induced conical intersection and berry phase," Phys. Chem. Chem. Phys. **23**, 16868 (2021).

[29] A. E. DePrince III, "Cavity-modulated ionization potentials and electron affinities from quantum electrodynamics coupled-cluster theory," J. Chem. Phys. **154**, 094112 (2021).

[30] M. Du, J. A. Campos-Gonzalez-Angulo, and J. Yuen-Zhou, "Nonequilibrium effects of cavity leakage and vibrational dissipation in thermally-activated polariton chemistry," J. Chem. Phys. **154**, 084108 (2021).

[31] T. S. Haugland, C. Schäfer, E. Ronca, A. Rubio, and H. Koch, "Intermolecular interactions in optical cavities: An *ab initio* study," J. Chem. Phys. **154**, 094113 (2021).

[32] J. Torres-Sánchez and J. Feist, "Molecular photodissociation enabled by ultrafast plasmon decay," J. Chem. Phys. **154**, 014303 (2021).

© Author(s) 2022

[33]I. V. Tokatly, "Time-dependent density functional theory for many-electron systems interacting with cavity photons," Phys. Rev. Lett. **110**, 233001 (2013).
[34]M. Ruggenthaler, N. Tancogne-Dejean, J. Flick, H. Appel, and A. Rubio, "From a quantum-electrodynamical light-matter description to novel spectroscopies," Nat. Rev. Chem. **2**, 0118 (2018).
[35]J. Flick and P. Narang, "*Ab initio* polaritonic potential-energy surfaces for excited-state nanophotonics and polaritonic chemistry," J. Chem. Phys. **153**, 094116 (2020).
[36]U. Mordovina, C. Bungey, K. Appel, P. J. Knowles, A. Rubio, and F. R. Manby, "Polaritonic coupled-cluster theory," Phys. Rev. Res. **2**, 023262 (2020).
[37]F. Buchholz, I. Theophilou, S. E. B. Nielsen, M. Ruggenthaler, and A. Rubio, "Reduced density-matrix approach to strong matter-photon interaction," ACS Photonics **6**, 2694–2711 (2019).
[38]J. Yang, Q. Ou, Z. Pei, H. Wang, B. Weng, Z. Shuai, K. Mullen, and Y. Shao, "Quantum-electrodynamical time-dependent density functional theory within Gaussian atomic basis," J. Chem. Phys. **155**, 064107 (2021).
[39]M. Ruggenthaler, F. Mackenroth, and D. Bauer, "Time-dependent Kohn-Sham approach to quantum electrodynamics," Phys. Rev. A **84**, 042107 (2011).
[40]M. Ruggenthaler, J. Flick, C. Pellegrini, H. Appel, I. V. Tokatly, and A. Rubio, "Quantum-electrodynamical density-functional theory: Bridging quantum optics and electronic structure theory," Phys. Rev. A **90**, 012508 (2014).
[41]C. Pellegrini, J. Flick, I. V. Tokatly, H. Appel, and A. Rubio, "Optimized effective potential for quantum electrodynamical time-dependent density functional theory," Phys. Rev. Lett. **115**, 093001 (2015).
[42]R. Jestädt, M. Ruggenthaler, M. J. T. Oliveira, A. Rubio, and H. Appel, "Light-matter interactions within the Ehrenfest-Maxwell-Pauli-Kohn-Sham framework: Fundamentals, implementation, and nano-optical applications," Adv. Phys. **68**, 225–333 (2019).
[43]C. L. Cortes, M. Otten, and S. K. Gray, "Non-Hermitian approach for quantum plasmonics," J. Chem. Phys. **152**, 084105 (2020).
[44]D. G. A. Smith, L. A. Burns, D. A. Sirianni, D. R. Nascimento, A. Kumar, A. M. James, J. B. Schriber, T. Zhang, B. Zhang, A. S. Abbott, E. J. Berquist, M. H. Lechner, L. A. Cunha, A. G. Heide, J. M. Waldrop, T. Y. Takeshita, A. Alenaizan, D. Neuhauser, R. A. King, A. C. Simmonett, J. M. Turney, H. F. Schaefer, F. A. Evangelista, A. E. DePrince III, T. D. Crawford, K. Patkowski, and C. D. Sherrill, "Psi4NumPy: An interactive quantum chemistry programming environment for reference implementations and rapid development," J. Chem. Theory Comput. **14**, 3504–3511 (2018).
[45]J. F. Stanton and R. J. Bartlett, "The equation of motion coupled cluster method. A systematic biorthogonal approach to molecular excitation energies, transition probabilities, and excited state properties," J. Chem. Phys. **98**, 7029 (1993).
[46]J. M. Turney, A. C. Simmonett, R. M. Parrish, E. G. Hohenstein, F. A. Evangelista, J. T. Fermann, B. J. Mintz, L. A. Burns, J. J. Wilke, M. L. Abrams, N. J. Russ, M. L. Leininger, C. L. Janssen, E. T. Seidl, W. D. Allen, H. F. Schaefer, R. A. King, E. F. Valeev, C. D. Sherrill, and T. D. Crawford, "Psi4: An open-source *ab initio* electronic structure program," Wiley Interdiscip. Rev.: Comput. Mol. Sci. **2**, 556 (2012).
[47]A. E. DePrince III, https://github.com/edeprince3/hilbert/, 2021; accessed 18 March 2022.
[48]J. McTague and J. J. Foley IV, https://github.com/psi4/psi4numpy/tree/master/Polaritonic-Quantum-Chemistry, 2021; accessed 18 March 2022.
[49]M. J. Perri and S. H. Weber, "Web-based job submission interface for the GAMESS computational chemistry program," J. Chem. Educ. **91**, 2206–2208 (2014).
[50]J. McTague and J. J. Foley IV, https://bit.ly/37GkzOz, 2021; accessed 17 March 2022.
[51]J. McTague and J. J. Foley IV, https://bit.ly/3KPvrYE, 2021; accessed 17 March 2022.
[52]J. McTague and J. J. Foley IV, https://bit.ly/37GmOBt, 2021; accessed 17 March 2022.
[53]J. McTague and J. J. Foley IV, https://bit.ly/3KPwyri, 2021; accessed 17 March 2022.
[54]J. McTague and J. J. Foley IV, https://bit.ly/3Jke0PF, 2021; accessed 17 March 2022.
[55]J. McTague and J. J. Foley IV, https://bit.ly/3qa5f39, 2021; accessed 17 March 2022.

© Author(s) 2022